

The Broadband Spectrum of Galaxy Clusters

Brandon Wolfe¹ and Fulvio Melia^{1,2}

ABSTRACT

We examine whether nonthermal protons energized during a cluster merger are simultaneously responsible for the Coma cluster’s diffuse radio flux (via secondary decay) and the departure of its intra-cluster medium (ICM) from a thermal profile via Coulomb collisions between the quasithermal electrons and the hadrons. Rather than approximating the influence of nonthermal proton/thermal electron collisions as extremely rare events which cause an injection of nonthermal, power-law electrons (the ‘knock-on’ approximation), we self-consistently solve (to our knowledge, for the first time) the covariant kinetic equations for the two populations. The electron population resulting from these collisions is out of equilibrium, yet not a power law, and importantly displays a higher bremsstrahlung radiative efficiency than a pure power law. Observations with GLAST will test this model directly.

Subject headings: acceleration of particles — galaxies: clusters: individual (Coma) — plasmas — radiation mechanisms: non-thermal — relativity — X-rays: galaxies

1. Introduction

Galaxy clusters, aggregates of more than 50 individual galaxies interspersed with a tenuous plasma known as the intracluster medium (ICM), are the largest gravitationally bound objects in the universe. Mergers of such clusters are the most energetic astrophysical events since the big bang: a merger of two $10^{15} M_{\odot}$ clusters releases some $10^{63} - 10^{64}$ ergs of gravitational energy.

Aside from providing heat (see, e.g., Brunetti et al. 2001; Ohno, Takizawa, & Shibata 2002; Fusco-Femiano et al. 1999; Rephaeli, Gruber, and Blanco 1999) observed as bremsstrahlung emission in the ICM (where the X-ray luminosity is typically $L_X \sim 10^{45}$ ergs

¹Physics Department, The University of Arizona, Tucson, AZ 85721

²Steward Observatory, The University of Arizona, Tucson, AZ 85721

s^{-1} , temperatures are in the range $\sim 2\text{--}10\text{ keV}$, and the central density is $\sim 10^{-3}\text{ cm}^{-3}$) such merger events also create supersonic shocks capable of accelerating nonthermal particles to energies greater than 1 TeV (Loeb & Waxman 2000). Examples of such shocks known to be ongoing in cluster mergers include the galaxy group NGC 4839, falling toward the center of the Coma cluster, as observed by XMM-Newton (Neumann et al. 2001). NGC 4839 achieves a velocity of $\sim 1,400\text{ km s}^{-1}$, and since the sound speed corresponding to Coma’s gas temperature of $\sim 8\text{ keV}$ is $\sim 1,000\text{ km s}^{-1}$, the subcluster’s supersonic motion is expected to produce shocks, which Neumann et al. (2001) claim to observe directly in the imaging of this cluster. Chandra observations of the ‘bullet’ cluster 1E 0657-558 (Markevitch 2002, 2004) show a prominent bow shock from a lower mass subcluster ($T \sim 6\text{ keV}$) as it exits the core of the main cluster ($T \sim 14\text{ keV}$) at a velocity of $4,500\text{ km s}^{-1}$. Within such shocks, some small fraction—typically $\sim 5\%$ (see, e.g., Berrington and Dermer 2005)—of the gravitational energy provided by the merger is believed to be converted into non-thermal particles through a first order Fermi (Drury 1985) process, although neither of the above cases provides direct evidence for such acceleration.

Further evidence for a population of accelerated, non-thermal particles coexisting with the thermal background ICM comes from diffuse radio emission extending over the entire $\sim 1\text{ Mpc}$ extent of certain rare clusters. Radio luminosities (polarized in at least one case), $L_r \sim 10^{40} - 10^{42}\text{ ergs s}^{-1}$, have been measured from emitting regions extending over a Mpc in 30 or so galaxy clusters (see, e.g., Kim et al. 1990; Giovannini et al. 1993; Giovannini & Feretti 2000; Kempner & Sarazin 2001). This emission—characterized as ‘halo’ if it is radially concentrated at the cluster center and ‘relic’ if instead it is located on the cluster’s outskirts—indicates synchrotron emission of relativistic electrons in a magnetized intracluster medium. Radio halos (such as the Coma cluster, which takes our focus here) further require a mechanism for constantly replacing energy lost by nonthermal electrons, since their radiative lifetimes (around 10^8 years) are too short to allow electrons to diffuse across the 100-kpc radio emitting region. The radial shape of halo emission, in particular, requires that nonthermal electrons be constantly created throughout the cluster.

One natural explanation (Dennison 1980) is that cosmic-ray protons, known to be confined within the cluster once produced—perhaps diffused throughout the cluster following a merger, although a central AGN (Blasi & Colafrancesco 1999) could also create sufficient non-thermal hadron energy—constantly collide with hydrogen and lose sufficient energy to create pions, which subsequently decay into the synchrotron-emitting electrons. However, due in part to difficulties reconciling this ‘secondary’ model with all multifrequency observations (Blasi and Colafrancesco 1999), it is often assumed electrons are constantly reaccelerated in situ by a second order Fermi mechanism (see, e.g., Blasi 2000).

In the Coma cluster and a dozen others (Dolag & Ensslin 2000), the diffuse radio emission exhibits a spectral break around 1GHz, with a steeper index at higher energy. Entire models have been based on this break, interpreted as the signature of electron escape (Rephaeli 1979), of a reacceleration of already relativistic electrons—possibly energized by a cluster merger event (Schlickeiser et al. 1987; Brunetti, Blasi, Cassano, and Gabici 2004)—or of energy-dependent radiative losses acting to impose a maximum electron energy during shock acceleration itself (Berrington & Dermer 2005; Webb, Drury & Biermann 1984; Dolag & Ensslin 2000). Notably, the secondary model we are proposing here does not reproduce this spectral steepening. Instead, it aims to reconcile past X-ray and future γ -ray observations using the simplest possible assumptions for the spectrum of accelerated particles, namely a pure power-law. The model posits that Coulomb collisions between the cluster’s high-energy proton population, and its thermal electrons, are the root of nonthermal excesses in the EUV and X-ray regimes. This is the novel component of this picture, replacing the ‘knock-on’ approximation with a full solution to the kinetics involved (see § 2).

Clusters produce an X-ray luminosity $L_X \sim 10^{45}$ ergs s^{−1}, generally interpreted as due to thermal bremsstrahlung by a tenuous thermal plasma characterized by a temperature in the range $\sim 2 - 10$ keV and a central density $\sim 10^{-3}$ cm^{−3}. These thermal X-ray emitting leptons coexist with the nonthermal radio-emitting leptons. Several clusters also display a slight excess above the thermal spectrum starting at $\sim 20 - 25$ keV and extending out to energies greater than ~ 45 keV. Though still somewhat controversial, this nonthermal component has thus far been reported for the Coma cluster (Fusco-Femiano et al. 1999; Rephaeli, Gruber, and Blanco 1999), Abell 2256 (Fusco-Femiano et al. 2000) and, most recently, for Abell 754 (based on long *Beppo*-SAX observations; Fusco-Femiano et al. 2003). Hard X-ray detections have been reported in several other Abell clusters (2199, 2319, and 3667) in the redshift range $0.023 < z < 0.056$, though apparently with weaker signals. Most of these excesses above the thermal emission can be fitted with a photon power-law spectrum and index ~ 2 . A recent example of this fitting procedure, applied to the RXTE source RX-J0658, may be found in Petrosian (2004).

An interpretation of the X-ray excess (HXR) as inverse Compton scattering (ICS) of synchrotron-emitting electrons breaks a degeneracy in the possible values of ICM magnetic field and electron energy (see, e.g., Rephaeli 1979). If the same electrons are responsible for both the radio synchrotron and nonthermal X-ray emission, then the implied magnetic field B must be an order of magnitude smaller than that observed. In the Coma cluster, for example, Faraday rotation measurements suggest that $B \sim 6 \mu\text{G}$ (Feretti et al. 1995), in sharp contrast with the value derived from *Beppo*-SAX observations (within the context of the inverse Compton scattering scenario), which instead require $B \sim 0.16 \mu\text{G}$ (Fusco-Femiano et al. 1999).

It can also be supposed that, in addition to the bremsstrahlung-emitting thermal ICM and synchrotron-emitting nonthermal electrons, a third nonthermal population of electrons exists which emits the X-Ray excess (HXR) as bremsstrahlung. Were such a population thermal, it would require a high temperature (> 50 keV), impossible to maintain against Coulomb re-equilibration if the species were not physically separated. Previously, Blasi (2000) suggested that hard X-ray emission in galaxy clusters may be due to bremsstrahlung radiation from a population of nonthermal electrons energized continuously out of the thermal pool via stochastic acceleration (see also Dogiel 2000; Sarazin and Kempner 2000; see also Liu, Petrosian, and Melia 2004 for a more recent treatment of this process). But the re-equilibration timescale of ~ 1 Myr, in the absence of an efficient energy-loss mechanism, means that all the energy given to the nonthermal component has been reprocessed into the thermal pool well before ~ 0.5 Gyr, heating the ICM above its observed temperature in less than 10^8 yrs (Petrosian 2001; Wolfe and Melia 2006b).

It was, however, suggested by Liang et al. (2002) and Dogiel et al. (2007) that a quasi-relativistic third population might overcome this difficulty via a higher radiative efficiency (and therefore a longer overheating time). Our model shares this characteristic, but rather than requiring a second-order Fermi acceleration to produce the quasi-relativistic particles, we assume they are produced via collisions with nonthermal protons. This appears to be quite natural, since it has long been believed that electrons accelerated via collisions with cosmic rays, known as ‘knock-on’ electrons, are more abundant than those produced by secondary decay in the ($\gamma_e < 100$) region (Schlickeiser 1999; Baring 1991). Our approach is simply to solve the kinetic equation of electrons, including both the standard terms (secondary injection, radiative losses, re-equilibration, etc.) and collisions with nonthermal protons. These protons are then simultaneously responsible for both the radio-emitting electrons and the nonthermal component of hard X-rays.

An additional motivation for this model is a somewhat controversial excess over the expected thermal bremsstrahlung that has been reported in the extreme ultraviolet (EUV): in Coma an excess was reported at 1.4×10^{-11} ergs cm $^{-2}$ s $^{-1}$ (Bowyer et al. 2004; Sarazin & Lieu 1998). Observations of an EUV excess have also been claimed in the Virgo and Abell clusters 1795, 2199, and 4059 (Durret et al. 2002). The standard interpretation for these observations is ICS of the cosmic microwave background by relativistic electrons. The EUVE measurement is curious because an ICS interpretation probes precisely the $10 > \gamma_e < 100$ portion of the electron distribution. Here, we show that secondary electrons alone cannot account for the EUVE, because the source function for electrons injected via proton-hydrogen scattering departs from a pure power-law at the relevant energies. We propose instead that the EUVE demonstrates the presence of electrons accelerated to high energies via proton-electron collisions.

By far the most significant motivating factor, however, is the possibility of observing γ -rays within a galaxy cluster. While no such observation has been confirmed (see, e.g., Reimer 2004), simple arguments (see below) show that a positive γ -ray flux from secondary decays in the Coma and other clusters should certainly lie within the sensitivity of the GLAST satellite telescope.

In nine years of observation, the EGRET satellite telescope gave only upper limits for the γ -ray flux of the most X-ray bright galaxy clusters, and it is here that our model receives its strongest test. In the case of the Coma cluster ($< 3.8 \times 10^{-8} \text{ cm}^{-2} \text{ s}^{-1}$; Reimer 2004), the γ -ray limit *excludes* the secondary model from consideration if the magnetic field within the cluster is $B < 1\mu\text{G}$ (Blasi & Colafrancesco 1999)—i.e., if the inverse Compton interpretation of the X-ray excess, and not Faraday rotation, correctly gives the magnetic field value—because a small magnetic field requires a detectably significant population of nonthermal hadrons.

Therefore, the significant contribution of the scenario we present here is the reconciliation of the secondary model with high magnetic field values and the X-ray excess, in the simplest possible manner. In this picture, cosmic-ray protons diffuse evenly throughout the cluster. They collide with hydrogen in the intracluster medium, producing a decay cascade whose products include electrons and γ -rays, each peaked at 70 MeV. These electrons, in magnetic fields $> 1\mu\text{G}$, produce diffuse radio emission. The cosmic-ray protons also collide with background thermal electrons and knock the tail of these electrons into a quasi-thermal third population. It is this third population, we believe, which is responsible for the EUV and hard X-ray excesses.

But this (perhaps still overly simplified) model notably fails to predict the spectral steepening at 1 GHz in Coma, as well as the radial dependence of the radio spectral index. The competing reacceleration model, in which already relativistic relic electrons are re-energized by a second-order stochastic acceleration process stirred by cluster mergers, already handles these details well. However, a non-ICS interpretation of the X-ray excess will become necessary should the GLAST satellite observatory, the HESS telescope—or others—confirm a positive γ -ray flux in the Coma cluster. The model presented here is a simple alternative which would be motivated mainly by such a positive detection.

2. Cosmic-Ray Kinetics

While our model proposes cosmic ray/electron (cr/e) collisions as a mechanism for producing the X-ray excess, it is important to stress a distinction between our approach

and the commonly used ‘knock on’ approximation (Abraham, Brunstein, and Cline 1966). That model was first proposed to describe an observed population of low-energy cosmic-ray electrons which exceeded the number expected from pion decay at the 70 MeV threshold. To make up for the discrepancy, cosmic ray/electron Coulomb collisions were proposed as a dominant mechanism for electron production in the $20 < \gamma_e < 200$ regime.

In the ‘knock on’ approximation, collisions are considered rare events which cause such radical change in the electron’s energy that electrons simply appear at the higher energy. Such injected electrons match the proton’s spectral index, at a rate proportional to the Coulomb cross-section for interaction (Baring 1991). Thus to account for the cr/e kinetics, one would need to break kinetics in two, with large-angle collisions represented as an injection $Q(u)$ and small-angle as the standard Boltzmann equation. More recently, however, complete covariant kinetic theories have appeared (Lifshitz & Pitaevskii 1958; Nayakshin and Melia 1998; Wolfe and Melia 2006b). If one were to break these theories into two parts at the outset—for small and large angles—one would find that the large-angle collisions are overwhelmed to the point of irrelevance (Nayakshin & Melia 1998), bringing the basic assumption of the Abraham, Brunstein, and Cline (1966) approximation into question. And besides, if cr/e collisions were in fact to provide a pure power-law injection, they would not be a candidate for producing Coma’s hard X-ray excess.

Particle collisions between protons and electrons cause the electrons to diffuse to higher energies, using a formalism very similar to the standard (Rosenbluth et al. 1957) theory. In that theory, the diffusion and advection of particles in velocity space are given by convolving the particle distribution with the kernels $|v-v'|$ and $|v-v'|^{-1}$. In the covariant generalization, these kernels must be corrected to (Landau 1936; Braams & Karney 1987; Wolfe & Melia 2006b)

$$D_{ab}(\mathbf{u}) = \frac{q_a^2 q_b^2}{m_a^2} \Lambda \int Z(u, u') f(u) du, \quad (1)$$

$$F_{ab}(\mathbf{u}) = \frac{q_a^2 q_b^2}{m_a m_b} \left(1 + \frac{m_a}{m_b} \Lambda \int \left(\frac{\partial}{\partial u} Z(u, u') \right) f(u) du \right). \quad (2)$$

Here and throughout $\mathbf{u} \equiv \gamma\beta c$ is the momentum in units of the rest mass.

Collisions between the nonthermal background of intracluster electrons, and nonthermal hadrons, are then solved via a coupled Fokker-Planck equation (see Wolfe and Melia 2006b). It is not difficult to understand how collisions develop the nonthermal electron distribution, especially in contrast with the ‘knock-on’ approximation which has, up to now, been used.

Baring (1991) holds that only large-angle collisions provide relativistic boosts to electrons, and this forms the basis of the ‘knock-on’ approximations’ philosophy. The Fokker-Planck equation including knock-on injection is a kind of Frankenstein monster which handles

e-p collisions once as a flux in the electron’s velocity space, and then again as a separate electron injection. But knock-on electrons are in fact proposed to describe relatively small jumps in energy, up to only $20 < \gamma_e < 200$, after which secondary production is expected to dominate. In writing the covariant Fokker-Planck equation, we have already made a small-angle assumption: consider instead Equation (13) in Melia & Nayakshin (1988) for the energy exchange rate before a small-angle assumption is made. As is shown in this paper, if one were to break this integral into a large and a small angles, the large-angle component, which represents ‘knock on’ electrons, would be vastly dominated by energy exchanged in small-angle collisions. Proton-electron collisions *do* produce nonthermal electrons. But they should be handled within the normal kinetic context, by supposing that such collisions require the solution of a coupled Fokker-Planck equation.

Inspection of the diffusion coefficient (Nayakshin and Melia 1998) for a thermal distribution of electrons and a power-law population of protons reveals that proton collisions dominate over electron collisions when the electron’s momentum is $p \sim m_e c/2$. This should be compared with the second-order Fermi diffusion coefficient used in previous studies (e.g., Blasi 2000). Collisional diffusion is less efficient, though of the same order, in the relevant energy range. Note that, while the power-law diffusion coefficient $D_{turb}(E) \sim E^\alpha$ will inevitably lead to a power-law tail for the electrons, the diffusion coefficient for collisions always falls to a constant, yielding a distribution which must go to zero. That is, collisions with a power-law distribution cannot themselves yield another power law. Unlike under the ‘knock-on’ approximation, electron collisions with power-law protons actually result in a nonthermal electron tail, steeper than the proton distribution, and featuring a hard cut-off at high energies. We call such electrons ‘quasi-thermal’.

Distinguishing quasi-thermal electrons from the power-law distributions produced by turbulent diffusion or under the traditional ‘knock-on’ approximation is essential, because their efficiency of bremsstrahlung emission is different (Liang et al. 2002; Dogiel et al. 2007).

3. Emission Types

Our actual calculation is time-dependent and exact. However, we may gain significant grasp of the model characteristics with a few simple analytic estimates. If we adopt the high-energy relation of Mannheim and Schlickeiser (1994) for the pion production rate of a power-law distribution of protons with index s ,

$$q_{\pi^0}(E_\pi) = q_{\pi^+}(E_\pi) = q_{\pi^-}(E_\pi) \sim 13.1 c n_{p0} n_H \sigma_{pp} \left[6(E_\pi/1 \text{ GeV}) \right]^{-(4/3)(s-1/2)}, \quad (3)$$

we may easily arrive at an approximate γ -ray source function,

$$q_\gamma(E_\gamma) = 2 \int_{E_\gamma + [m_\pi c^2 / (4E_\gamma)]}^{\infty} dE_\pi q_{\pi^0}(E_\pi) [E_\pi^2 - m_\pi^2 c^4]^{-1/2}, \quad (4)$$

which we may safely expect (Markoff, Melia, and Sarcevic 1997; Fatuzzo and Melia 2003; Crocker et al. 2005) will also approximate the number of neutrinos injected per unit volume, per unit time (both in the high-energy limit). Meanwhile, the rate of electron injection is

$$\begin{aligned} q_e &= \frac{m_\pi}{70 m_e} q_{\pi^\pm} \left(\frac{E_\pi}{70 \text{ MeV}} \right) \sim \frac{13}{12} \sigma_{pp} c n_H n_{p0}(r) \left(\frac{m_p}{24 m_e} \right)^{s_{e0}-1} (\gamma_e \beta_e)^{-s_{e0}} \text{ cm}^{-3} \text{ s}^{-1} \\ &\equiv K_{inj} \gamma_e^{-s_{e0}}, \end{aligned} \quad (5)$$

where the electron spectral index $s_{e0} = (4/3)(s - 1/2)$ matches that of the pions. We find that these approximations are valid to within a factor 3 above the threshold energy for pion production at 70 MeV (Markoff, Melia, and Sarcevic 1997).

Assuming the dominant loss mechanism is either inverse Compton scattering with a blackbody photon background ($T_{CMB} = 2.73 \text{ K}$), or radio synchrotron (Wolfe and Melia 2006a), radiative losses are given by $-dE_e/dt = a_s E_e^2$, with the constant $a_s = (4/3)\sigma_T c n_e (\epsilon_{CMB} + \epsilon_B)/m_e c^2$. The energy density (ϵ_{CMB}) in the CMB dominates (by over a decade) over that (ϵ_B) in the magnetic field. The equilibrium distribution of electrons due to injection against these losses is

$$n(\gamma_e) = \frac{K_{inj}}{m_e c^2 a_s (s_{e0} - 1)} \gamma_e^{-(s_{e0}+1)}. \quad (6)$$

The radio synchrotron emissivity (in units of energy per unit volume, per unit time, per unit frequency) associated with this distribution is then

$$\frac{dE}{dV d\nu dt} \approx 1.15 \pi^2 \frac{K_{inj} \alpha \hbar \nu_B}{m_e c^2 a_s (s_{e0} - 1)} \left(\frac{\nu_B}{\nu} \right)^{s_{e0}/2}, \quad (7)$$

where ν_B is the gyrofrequency, and the corresponding Compton scattering emissivity off the CMB (in units of photon number per unit volume, per unit time, per unit energy) is

$$\frac{dN_\gamma}{dV d\epsilon dt} = 1.8 \frac{r_0^2}{\hbar^3 c^2} \frac{K_{inj}}{m_e c^2 a_s (s_{e0} - 1)} (kT_{CMB})^{(s_{e0}+6)/2} \epsilon^{-(s_{e0}+2)/2}, \quad (8)$$

where r_0 is the classical electron radius, and we have used the fact that the hard X-radiation is produced below the Klein-Nishina region to simplify the cross section. Note that, while the synchrotron emissivity varies roughly as the square of the magnetic field, inverse Compton scattering depends only on the relative normalization K_{inj} of electrons required for consistency with radio observations.

Finally, thermal bremsstrahlung emission in the relativistic region is approximated using a Gaunt factor (Rybicki & Lightman 1985) representing the multiplicative difference between quantum-nonrelativistic and QED (Haug 1997) bremsstrahlung cross-sections. It may be reconstructed to better than $\sim 5\%$ accuracy as

$$\bar{g}_{ff}(\phi) = A \log(\phi) + B + C\phi^D + E\phi^F \quad (9)$$

where A through F are functions of θ alone,

$$\begin{aligned} A, B, E, \&F &= a_i \theta^{b_i} + c_i \theta^{d_i} + e_i \\ D &= 1.95 \\ C &= a_5 \theta^{b_5} + c_5 \theta^{d_5} \exp(-e_5 \theta), \end{aligned} \quad (10)$$

and where $\phi = h\nu/kT$ and $\theta = kT/m_e c^2$. These coefficients are given in Table 1.

4. Model Characteristics

Our guide for reasonable magnetic fields, particle densities, etc. is both a simultaneous fit of multifrequency observations, and a maximum total energy budget being the power dissipated in a central merger event between two clusters of mass M , which is

$$L_p \sim 0.1 \frac{GM^2}{R_{sh} t_{cl}} \sim 10^{44} \text{ ergs s}^{-1}, \quad (11)$$

where the shock radius R_{sh} is ~ 5 Mpc, and the cluster's age $t_{cl} \sim 10^{10}$ yr.

Assuming an ICM gas mass $M_{gas} \sim 10^{14} M_\odot$ and a total cluster mass $M_{tot} \sim 10^{15} M_\odot$, over an active distance comparable with the Abell radius, the average ICM gas density is $n_H \sim 3 \times 10^{-4} \text{ cm}^{-3}$. We adopt a magnetic field $B = 0.8 \mu\text{G}$, which would underproduce inverse Compton scattered photons at the X-ray excess by roughly two orders of magnitude. We accept a recent estimate for the Coma's distance of 102 Mpc; at a bremsstrahlung temperature $T = 8.21 \text{ keV}$, the measured X-ray luminosity then implies an active volume $\sim 1.5 \text{ Mpc}^3$. Finally, we take the spectral index s_p of the proton distribution $n_p = n_{p0}(\gamma\beta)^{-s_p}$ to have the value 2.1. The end result is a nonthermal hadron population consistent with a cosmic ray luminosity $L_p = 4.5 \times 10^{43} \text{ ergs s}^{-1}$, within the energy budget of a cluster merger.

5. Particle Distribution Function and Broadband Flux

We show the evolution of the quasi-thermal component of the electron distribution in Fig. 1a, together with bounding thermal distributions to demonstrate its non-thermal character. The power-law tail is most pronounced after only $10^7 - 10^8$ years; however, the efficient

energy loss via electron-proton collisions (bremsstrahlung) prevents rapid overheating and leads to a quasi steady-state distribution. Evolution of the nonthermal component is shown in Fig 1b: while the high-energy component assumes essentially the form of a pure power-law injection subject to synchrotron losses, the pion threshold region rapidly thermalizes.

Radio synchrotron emission (Fig. 2a) comes from the purely power-law component of injected electrons. Clusters require at least some 100 Myr to reach their steady state, characterized by a power-law index one greater than the injection index. Nonthermal X-ray bremsstrahlung (Fig. 2b) shows an excess consistent with that observed via *Beppo-SAX* (Fusco-Femiano et al. 2004), although less consistent with the RXTE (Rephaeli & Gruber 2002) observations. As expected, ICS emission falls well below the required excess with any magnetic field $\sim 1\mu\text{G}$.

The reported EUV excess (Bowyer et al. 2004; Sarazin & Lieu 1998) cannot be due to inverse Compton scattering of CMB photons by the nonthermal component of secondary electrons, because this emission comes from the threshold region, and where Coulomb losses dominate. Even supposing a magnetic field of $0.2\mu\text{ G}$, the inverse Compton flux at 2×10^2 eV falls several decades short of the excess power reported by Bowyer et al. (2004) (see Fig. 3).

The detection limits of EGRET and GLAST straddle the 70 MeV pion bump, so it is worthwhile improving upon the rough sketch we have outlined above for the γ -ray emissivity, by considering a more exact treatment. In Fig. 4 we display the γ -ray flux consistent with both the diffuse radio and X-ray emission. For energies above $E_\gamma > 100$ MeV, the approximation (thin solid line) holds well. Note that the γ -ray luminosity produced by nonthermal electron-proton bremsstrahlung is always several decades below that produced via pion decay.

6. Conclusions

Previously (Liang et al. 2002; Dogiel 2006) it was shown that, because the efficiency of bremsstrahlung emission for a quasithermal distribution is decades higher than for a pure power law (Petrosian 2001), this type of distribution may account for the nonthermal X-ray excess. However, it was believed that proton collisions did not qualify, since under the ‘knock-on’ approximation they produce electrons in a power law. Here, by solving the covariant kinetics self-consistently, we have shown that collisions do create a suitable quasithermal distribution. As further motivation that nonthermal proton/ quasi-thermal electron collisions are in fact relevant in clusters, we have shown that electrons injected during proton

collisions may not account for the EUV excess via inverse Compton scattering with the CMB, because the relevant injection occurs below the 70 MeV pion bump.

Describing the X-ray excess as due to a quasi-thermal electron population allows us to model the Coma cluster of galaxies using a value for the magnetic field in the intra-cluster medium which agrees with that given by Faraday rotation measurements. Luckily, our model has a near-term litmus test via the GLAST satellite: the resolution of γ -rays from the Coma cluster would demonstrably prove the presence of nonthermal hadrons and require a secondary model which could describe radio, X-ray, and γ -ray observations simultaneously. A null detection would favor the ICS interpretation of an X-ray excess, meaning that a secondary model for radio emission in Coma cannot be correct. Whatever the outcome, we suggest that problems which invoke the ‘knock-on’ approximation would benefit considerably from a treatment using covariant kinetics, as we have developed here and in our previous work (Wolfe and Melia 2006b).

This research was supported by NSF grant AST-0402502 at the University of Arizona.

REFERENCES

- Abraham, P. B., Brunstein, K. A., and Cline, T. L., 1966, *Phys. Rev.*, 150, 1088
- Baring, M., 1991, *MNRAS*, 253, 388
- Berrington, R. C. and Dermer, C. C., 2003, *ApJ*, 594, 709
- Blasi, P., 2000, *ApJL*, 532, L9
- Blasi, P. and Colafrancesco, S., 1999, *Astropart. Phys.*, 12, 169
- Bowyer, S., Korpela, E. J., Lampton, M., and Jones, T. W., 2004, *ApJ*, 605, 168
- Braams, B. J. and Karney, C. F., 1987, *PRL*, 59, 1817
- Brunetti, G., Setti, G., Feretti, L., and Giovannini, G., 2001, *MNRAS*, 320, 365
- Brunetti, G., Blasi, P., Cassano, R., and Gabici, S., 2004, *MNRAS*, 350, 1174
- Crocker, R. M. et al., 2005, *ApJ* 622, 892
- Dennison, B., 1980, *ApJ*, 239, L93
- Dogiel, V. A., 2000, *AA*, 357, 66

- Dogiel, V. A. et al., 2007, *A&A*, 461, 433
- Drury, L. O’D., 1985, in *Cosmical gas dynamics*, VNU Science Press, Utrecht, p. 131
- Dolag, K. and Ensslin, T. A., 2000, *A&A*, 362, 151
- Durret, F., Slezak, E., Lieu, R., Dos Santos, S., and Bonamente, M., 2002, *A&A*, 390, 397
- Fatuzzo, M. and Melia, F., 2003, *ApJ*, 596, 1035
- Feretti, L., Dallacasa, D., Giovannini, G., and Tagliani, A., 1995, *AA*, 302, 680
- Fusco-Femiano, R., Dal Fiume, D., Feretti, L. et al. 1999, *ApJL*, 513, L21
- Fusco-Femiano, R., Dal Fiume, D., De Grandi, S. et al. 2000, *ApJL*, 534, L10
- Fusco-Femiano, R., Orlandini, M., De Grandi, S. et al. 2003, *AA*, 398, 441
- Giovannini, G., Feretti, L., Venturi, T., Kim, K.-T., Kronberg, P. P., 1993, *ApJ*, 406, 399
- Giovannini, G. and Feretti, L., 2000, *New Astronomy*, 5, 335
- Haug, E. 1997, *A&A*, 326, 417
- Kempner, J. C. and Sarazin, C. L. 2001, *ApJ*, 548, 639
- Kim, K.-T., Kronberg, P. P., Dewdney, P. E., and Landecker, T. L., 1990, *ApJ*, 355, 29
- Landau, L. D., 1936, *Physik. Zeits. Sowjetunion*, 10, 154
- Liang, H., Dogiel, V. A., and Birkinshaw, M., 2002, *MNRAS*, 337, 567
- Lifshitz, E. M. and Pitaevskii, L. P., 1958, *Sov. Phys. JETP*, 6, 418
- Liu, S., Petrosian, V., and Melia, F., 2004, *ApJL*, 611, L101
- Loeb, A. and Waxman, E., 2000, *Nature*, 405, 156
- Mannheim, K. and Schlickeiser, R., 1994, *A&A*, 286, 983
- Markevitch, M. et al., 2002 *ApJL*, 567, L27
- Markevitch, M. et al., 2004, *ApJ*, 606, 819
- Markoff, S, Melia, F., and Sarcevic, I., 1997, *ApJ*, 489, L47
- Nayakshin, S. and Melia, F., 1998, *ApJS*, 114, 269

- Neumann, D. M. et al., 2001, *A&A*, 365, 74
- Ohno, H., Takizawa, M., and Shibata, S., 2002, *ApJ*, 577, 658
- Petrosian, V., 2001, *ApJ*, 557, 560
- Petrosian, V., 2004, 35th COSPAR Scientific Assembly, 4202
- Reimer, O., 2004, *Journal of the Korean Astronomical Society*, 37, 307
- Rephaeli, Y., 1979, *ApJ*, 227, 364
- Rephaeli, Y., Gruber, D.E., and Blanco, P., 1999, *ApJL*, 511, L21
- Rosenbluth, M.N., MacDonald, W.M., Chuck, W., 1957, *Phys. Rev.*, 107, 350
- Rybicki, G. and Lightman, A., 1985, *Radiative Processes in Astrophysics* (Wiley: NY)
- Sarazin, C.L. and Kempner, J.C., 2000, *ApJ*, 533, 73
- Sarazin, C. L. and Lieu, R., 1998, *ApJL*, 494, L177
- Schlickeiser, R., 1999, *A&A*, 351, 382
- Schlickeiser, R., Sievers, A., and Thiemann, H., 1987, *AA*, 182, 21
- Webb, G. M., Drury, L. O’C., and Biermann, P., 1984, *A&A*, 137, 185
- Wolfe, B. and Melia, F., 2006a, *ApJ*, 637, 313
- Wolfe, B. and Melia, F., 2006b, *ApJ*, 638, 125

Table 1: Electron-Proton Thermal Gaunt Factor Expansion Coefficients

	c_{i0}	c_{i1}	c_{i2}	c_{i3}	c_{i4}	c_{i5}	c_{i6}
c_{0j}	9.380e-04	1.924e-03	-3.726e-03	-9.218e-03	-1.011e-04	8.037e-03	4.182e-03
c_{1j}	8.654e-04	-4.263e-04	-1.128e-02	-1.273e-02	1.150e-02	2.236e-02	5.062e-03
c_{2j}	-7.215e-03	-1.803e-02	1.731e-02	6.562e-02	1.929e-02	-4.031e-02	-3.520e-02
c_{3j}	-3.194e-03	6.941e-03	6.072e-02	5.678e-02	-7.306e-02	-1.248e-01	-2.687e-02
c_{4j}	2.083e-02	5.496e-02	-4.063e-02	-1.892e-01	-7.899e-02	9.842e-02	1.279e-01
c_{5j}	-1.647e-03	-3.669e-02	-1.110e-01	-3.922e-02	2.015e-01	2.558e-01	2.765e-02
c_{6j}	-2.376e-02	-5.335e-02	8.173e-02	2.419e-01	4.259e-02	-2.123e-01	-2.705e-01
c_{7j}	1.549e-02	6.619e-02	5.372e-02	-1.291e-01	-2.818e-01	-2.152e-01	1.662e-01
c_{8j}	1.368e-03	-2.695e-02	-1.052e-01	-2.340e-02	3.103e-01	5.121e-01	8.041e-01
c_{9j}	-1.703e-02	-5.764e-02	1.883e-02	2.948e-01	4.358e-01	7.627e-02	2.455e-01

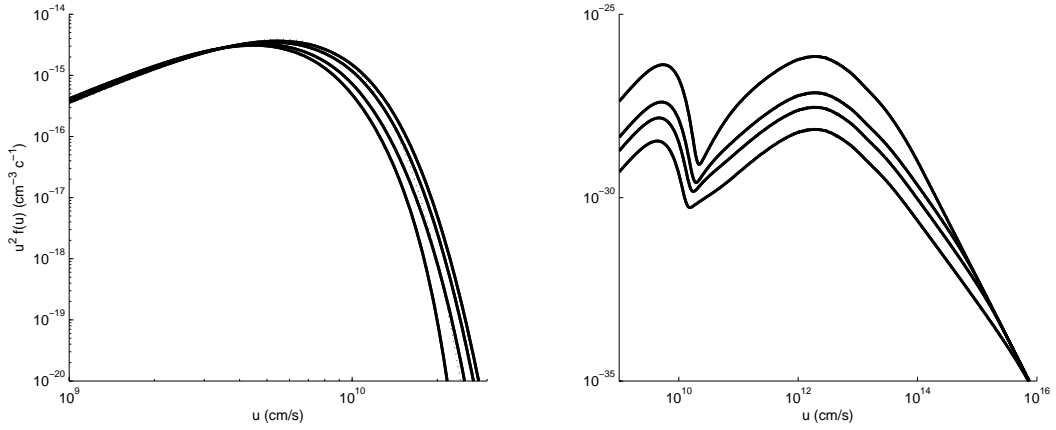


Fig. 1.— Thermal background electrons (panel a, on the left) at $t = 5, 20, 102$, and 650 Myr (left to right) are given a nonthermal tail which is most pronounced within 10 Myr, but which is maintained in a quasi steady-state for upwards of 1 Gyr. A thermal distribution at $T = 8.21$ keV would lie just inside of the curve at $t = 5$ Myr. Nonthermal secondary electrons (panel b, on the right), at identical times (bottom to top), feature a spectral break due to ICS losses which by 650 Myr encompasses the energies observed via radio synchrotron. Electron injection at $E_e < 1$ GeV is limited by the threshold bump, as well as by Coulomb losses into a thermal population (note the downward curvature near $u = c$ of depleted electrons by 650 Myr).

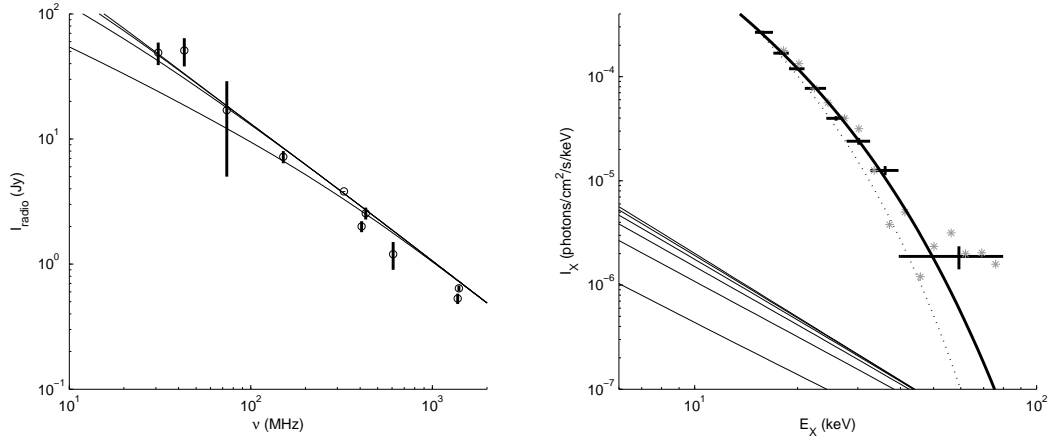


Fig. 2.— A comparison of the observed diffuse radio emission (panel a, on the left) below the 1.4 GHz spectral break, with the calculated synchrotron emissivity at $t = 50, 100, 150$, and 200 Myr, indicates that the injection must be ongoing for at least 100 Myr. After this time, the distribution has reached its steady state. Diffuse X-ray emission (panel b, on the right) from nonthermal electrons at 650 Myr accounts for the observed hard X-radiation (the histogram is from *Beppo-SAX*, the points are from *RXTE*)—whereas, at $B = 0.8 \mu\text{G}$, inverse Compton scattered radiation (solid lines to the bottom left of this panel, shown at times coincident with Fig. 2a) is an order of magnitude below the hard X-rays. The contribution from a thermal distribution at $T = 8.21$ keV (dotted) is presented for comparison.

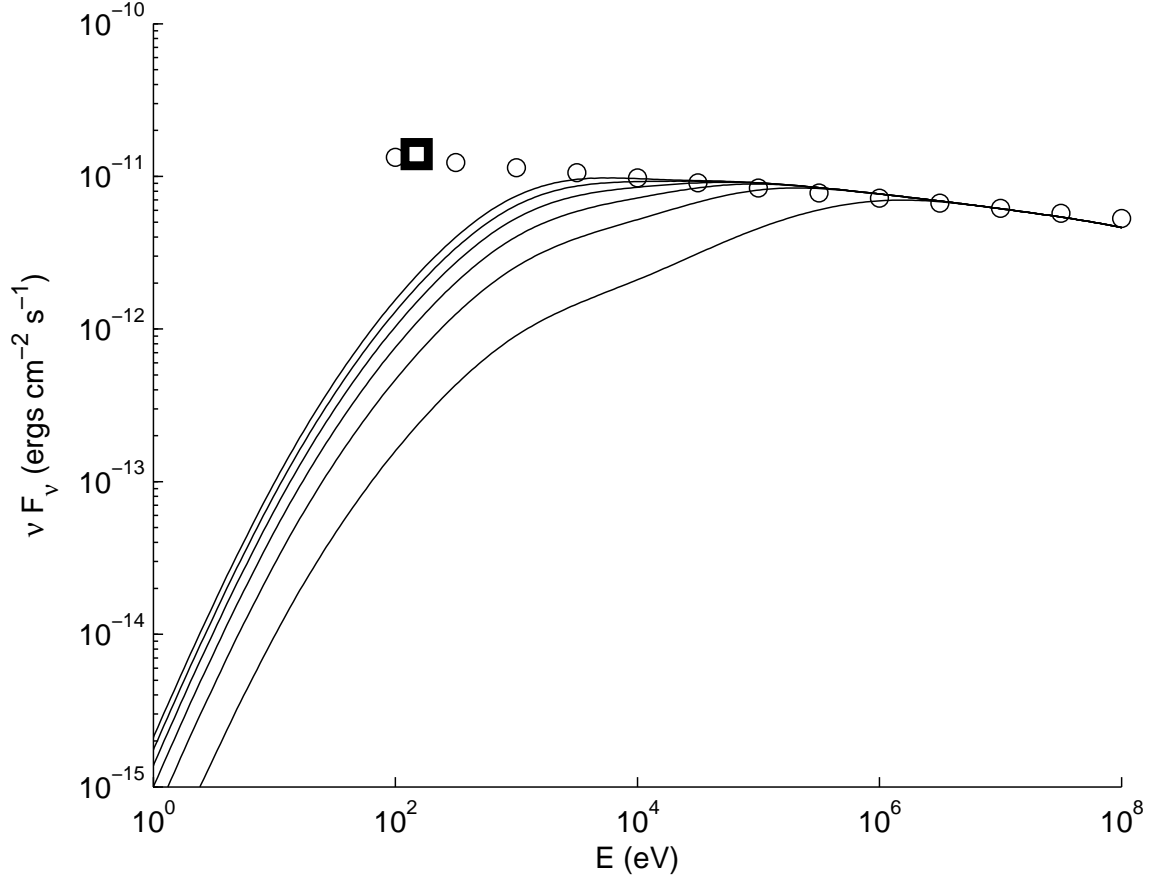


Fig. 3.— Even supposing a magnetic field of $0.16 \mu\text{G}$, inverse Compton scattering emission from secondary electrons cannot account for the EUV excess (shown here as a heavy box). The emissivity due to the self-consistent electron distribution (at $t = 50, 150, 250, 350, 450,$ and 550 Myr) falls below the naive expectation (shown here as circles) as a result of the pion threshold and Coulomb losses.

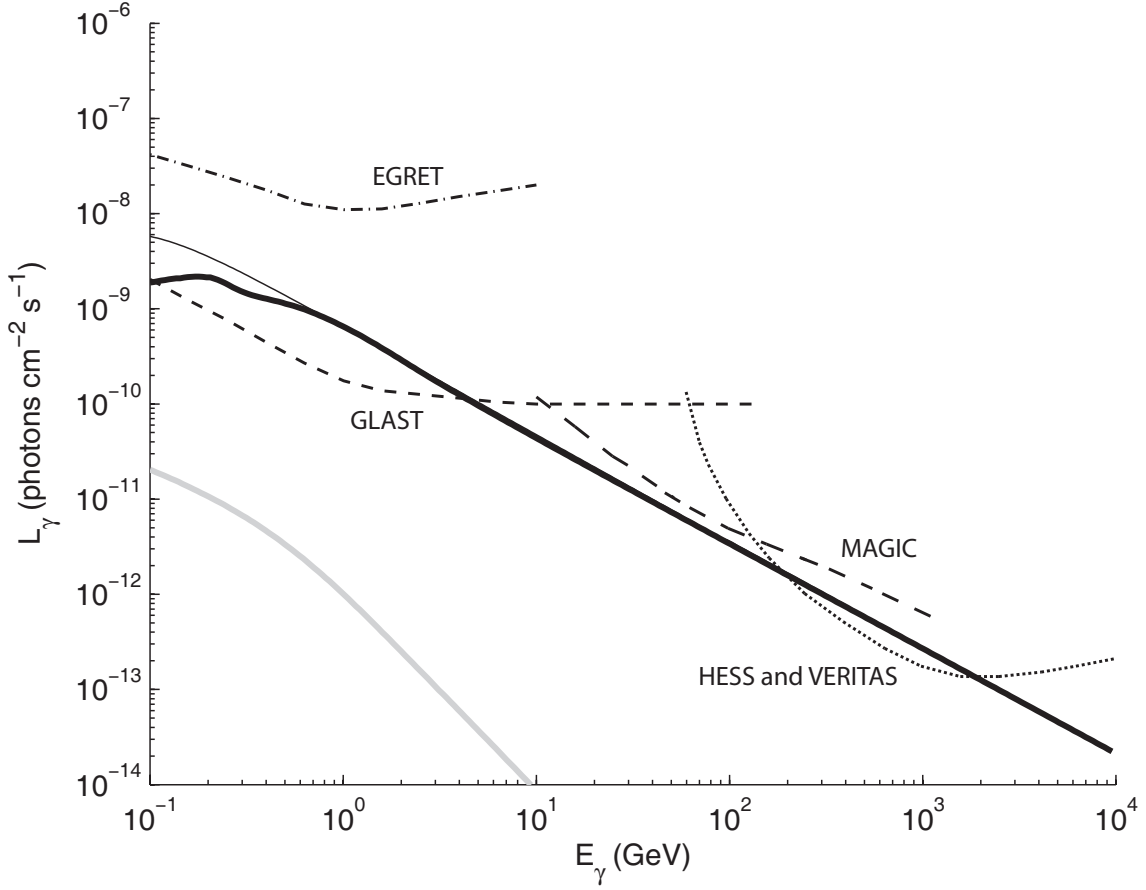


Fig. 4.— Predicted secondary γ -ray emission due to proton-proton scattering within the Coma cluster. Sensitivity limits for EGRET (dot-dash), MAGIC (long dash), GLAST (short dash), and VERITAS and HESS (dot) (DB05) are also presented. Bremsstrahlung from the nonthermal electron component (shaded solid) is always well below detection.